ANNALS OF GEOPHYSICS, SUPPLEMENT TO VOL. 47, N. 2/3, 2004

11

Investigation into the problem of characterization of the HF ionospheric fluctuating channel of propagation: construction of a physically based HF channel simulator

VADIM E. GHERM ([1]), NIKOLAY N. ZERNOV ([1]) and HAL J. STRANGEWAYS ([2])

([1]) *University of St. Petersburg, Russia*
([2]) *School of Electronic and Electrical Engineering, University of Leeds, U.K.*

A wideband HF simulator has been constructed that is based on a detailed physical model. It can generate an output giving a time realization of the HF wideband channel for any HF carrier frequency and bandwidth and for any given transmitter receiver path, time of day, month and year and for any solar activity/geomagnetic conditions. To accomplish this, a comprehensive solution has been obtained to the problem of HF wave propagation for the most general case of a 3D inhomogeneous ionosphere with time-varying electron density fluctuations. The solution is based on the complex phase method (Rytov's method), which has been extended to the case of an inhomogeneous medium and a point source of the field. Results of simulation obtained according to the technique developed have been presented, calculated for a single-hop path 1000 km long oriented to the south from St. Petersburg and including a horizontal electron density gradient present in the IRI model used as the basis of the ionosphere model. The fluctuations of the ionospheric electron density were characterized by an inverse power law anisotropic spatial spectrum. For this model, the random walk of the phasor at the receiver is determined and shown both for paths reflected in the *E*- and *F*-regions, being significantly larger for the latter. The oblique sounding ionogram is constructed and reveals three propagation modes: the *E*-mode and low and high angle *F*-mode paths. The time-varying field due to each of these paths is then summed at the receiving location enabling the calculation of the scattering function and also the time realization of the received signal shown as a function of both fast and slow time. This is performed both with and without the presence of the geomagnetic field; in the former case the splitting of the *F*2-mode into both *e*- and *o*-modes is seen. It is also shown how the scattering function can be obtained from the time realization of the channel in a way akin to experimental determination of the scattering function from channel measurements. Results from the simulations show the very significant effect of irregularities of even modest magnitude and the comparative effects due to background ionosphere dispersion and the fluctuating irregularities as well as geomagnetic mode splitting. Since the simulator is based on a physical model, it should be possible by comparison of experimental results and simulation to identify the correspondence between physical parameters (*e.g.,* the variance and anisotropy of the electron density fluctuations, orientation of the propagation path to the magnetic meridian, bulk ionosphere motions) with observed channel parameters (*e.g.,* Doppler spread and shift, time delay spread).

11.1. INTRODUCTION

To properly characterize the ionospheric reflection HF fluctuating channel of propagation on a physical basis, a comprehensive solution should be devised to solve the problem of high frequency wave propagation in the 3D inhomogeneous (rigorously also anisotropic) ionosphere with local random inhomogeneities embedded. This entails a comprehensive solution to the problem of wave propagation in a random medium for the most general case of a 3D inhomogeneous dispersive medium with fluctuations of the parameters including the case of strong scintillation (strong fluctuation of the field amplitude), or that of the saturated regime of propagation. Although a rigorous solution to this problem is not currently available, we consider the best available solution that is based on the complex phase method (in classical terms, Rytov's method), which we have extended to the case of an inhomogeneous medium and a point source of the field.

First, Zernov (1980) extended this method to the case of a plane-layered background medium and a point source. This permits simultaneous accounting for the ray bending and the scattering by local random inhomogeneities, including diffraction effects on local inhomogeneities. This extension was intensively employed in a series of papers (Gherm and Zernov, 1995; Gherm *et al*., 1997a,b; Gherm and Zernov, 1998; Gherm *et al*., 2001a,b, 2002, 2003) to study effects due to fluctuations of the electron density in the plane-stratified ionosphere. Gherm and Zernov (1995) studied the statistical moments of the phase and log-amplitude of the HF field, in particular, the effect of Fresnel filtering. Subsequent papers (Gherm *et al*., 1997a,b) were devoted to the effects on propagation of both narrow- and wideband pulses in the fluctuating ionosphere. Moments of the full field in the HF-band, in particular the scattering function, were studied in a series of papers (Gherm and Zernov, 1998; Gherm *et al.*, 2000, 2001a,b, 2002). A review paper on HF propagation in the ionosphere disturbed by random inhomogeneities was subsequently given at the 27th General Assembly of URSI in Maastricht, The Netherlands by Zernov *et al*. (2002). However, all the investigations described were limited by a plane-stratified isotropic model of the background ionosphere.

It was then considered important to extend the complex phase method to the case of a 3D inhomogeneous background medium, which is necessary, in particular, to account for the effects of a horizontally inhomogeneous background ionosphere. This extension was made by Gogin *et al.* (2001) and thus enables the widening of the range of possible conditions of the HF propagation in the ionosphere. Finally, the most general theory was developed in the scope of the Project «Wideband HF and UHF simulators for ionosphericaly reflected transionospheric channels», (under the financial support of the U.K. EPSRC Visiting Fellowships programme, grant GR/R37517/01) where the effects of the anisotropy of the ionosphere (including the background ionosphere) were taken into account. This project was performed in collaboration between the University of St. Petersburg, St. Petersburg, Russia (NNZ and VEG) and the University of Leeds, Leeds, U.K. (HJS).

This investigation resulted in producing a physically based software simulator for the HF ionospheric reflection fluctuating channel of propagation which overcame limitations of empirically based models such as that developed by Mastrangelo *et al.* (1997) on the basis of the work by Vogler and Hoffmeyer (1993). This simulator requires a large number of input parameters for each propagation mode which cannot be directly determined from the parameters of the transmission path and model ionosphere. Further, it is also based on a limited amount of data for an undisturbed ionosphere and it is rather questionable whether extrapolation to disturbed ionosphere conditions is valid. The basis for the delay profile modelling which is the main difference from the Watterson model is also not clear.

To overcome these and other limitations, the wideband HF simulator constructed is based on a detailed physical model. It can generate an output giving a time realisation of the HF channel (as well as the statistical moments of a signal, *e.g.,* the scattering functions) for any bandwidth (up to a MHz) and for any given time, path and conditions. To characterise the HF channel of propagation, an analytic-numerical technique has been used, which employs the complex phase method, which, as was just

mentioned, was recently extended to the case of a 3D inhomogeneous and even anisotropic medium. The main principles of constructing this physically based software simulator will be outlined below.

11.2. Main relationships

It is assumed that a random realization of a pulsed signal propagated through the fluctuating ionosphere is represented as the following Fourier integral in the frequency domain:

$$U(\boldsymbol{r},t,T)=\sum_{m}\int_{-\infty}^{+\infty}P(\omega)\,E_{0m}^{\mathrm{GO}}(\boldsymbol{r},\omega)\,R_{m}(\boldsymbol{r},\omega,T)\,e^{-i\omega t}\,d\omega. \tag{11.1}$$

Here $P(\omega)$ is the spectrum of a launched pulse, E_{0m}^{GO} represents the transfer function for a given m-th path in the undisturbed channel, where the field in the undisturbed channel is represented by the sum

$$E_{0}(\boldsymbol{r})=\sum_{m}E_{0m}^{\mathrm{GO}}(\boldsymbol{r}) \tag{11.2}$$

of the geometrical optics type fields E_{0m}^{GO}, each propagating from a source to a receiver along its own path of propagation. Once the model of the 3D background ionosphere is given, quantities E_{0m}^{GO} are calculated employing the appropriate ray-tracing code, which also permits calculation of the ray tube divergence. Accepting representation (11.2) for the undisturbed field implies a limitation to cases where the observation points are far from any caustic (*i.e.* far from the skip distance, if the transmitter and receiver are located on the Earth's surface).

The random phasor $R_m(\boldsymbol{r},\omega,T)$ is introduced in (11.1) to account for the effects of fluctuations of the electron density of the ionosphere. Variable t is the flight time of a pulse and T denotes the slow time dependence of fluctuations, which can be treated in the *quasi*-stationary approximation. The background channel is assumed to be stationary; that is time independent. A corollary of this is the absence of slow time dependence in the transfer functions of the background channel in (11.2). The summation in (11.2) is performed over all paths of propagation from a transmitter to a receiver.

According to the complex phase method, random phasors $R_m(\boldsymbol{r},\omega,T)$ are represented utilising complex phases as follows:

$$R_{m}(\boldsymbol{r},\omega,T)=\exp\left[\psi_{m}(\boldsymbol{r},\omega,T)\right] \tag{11.3}$$

where the first and second order complex phases ψ_m, in powers of the disturbances of the dielectric permittivity of the medium of propagation, are utilised in the following consideration. Complex phases

$$\psi_{m}(\boldsymbol{r},\omega,T)=\chi_{m}(\boldsymbol{r},\omega,T)+iS_{m}(\boldsymbol{r},\omega,T) \tag{11.4}$$

are random functions with the real part χ_m representing log-amplitude fluctuations and S_m giving the fluctuations of the phase of the field. Thus, eqs. (11.1) to (11.4) comprise the formal basis to produce both the random time series (sequences) of the pulsed signal (11.1) and its statistical moments, *e.g.,* the scattering functions. Analytical expressions for $\psi_m(\boldsymbol{r},\omega,T)$ can be found in Gogin *et al.* (2001).

The appropriate statistical moments of the log-amplitude and phase, which are necessary to produce both random series of a signal and its scattering function, are constructed and calculated in ray-centred variables associated with every path of propagation in the background medium, linking the transmitter and receiver. These paths are constructed by means of the numerical ray-tracing for the background ionosphere. Numerical rather than analytic ray-tracing (*e.g.*, using the multi-*quasi*-parabolic model) is required since the effect of the geomagnetic field is included to determine both *o*- and

e-modes and also to find paths through any 3D ionosphere model including horizontal gradients. The presence of some local deterministic inhomogeneities (*e.g.,* TIDs) or regular Doppler shifts due to bulk motion of the ionosphere can also be accounted for. Oblique sounding ionograms are constructed which are then employed to specify the possible paths of propagation between the given transmitter and receiver locations, so that multi-path effects are taken into account. Each propagation path for each magneto-ionic mode is determined by employing a homing-in procedure using the Nelder-Mead algorithms (Strangeways, 2000) together with the 3D ray-tracing program.

11.3. PRODUCTION OF RANDOM TIME SERIES

To produce time series of a pulsed signal given by the Fourier integral (11.1) for a point of observation r, two real random functions χ_m and S_m must be generated in a two dimensional domain (ω, T) for a given value of $\boldsymbol{r}$. This demands knowledge of the probability density functions for χ_m and S_m, as well as their auto- and cross-correlation functions. In the scope of the complex phase method, these functions are given as follows:

$$B_\chi(\omega_1, \omega_2; T_1, T_2) = \left\langle \chi_1(\omega_1, T_1)\, \chi_1(\omega_2, T_2) \right\rangle \tag{11.5}$$

$$B_s(\omega_1, \omega_2; T_1, T_2) = \left\langle S_1(\omega_1, T_1)\, S_1(\omega_2, T_2) \right\rangle \tag{11.6}$$

$$B_{\chi s}(\omega_1, \omega_2; T_1, T_2) = \left\langle \chi_1(\omega_1, T_1)\, S_1(\omega_2, T_2) \right\rangle. \tag{11.7}$$

According to the complex phase method, quantities χ_{m1} and S_{m1} are represented by linear integrals over many random inhomogeneities. This guarantees, according to the central limit theorem, a normal distribution for both the random functions χ_{m1} and S_{m1}. When averaging in eqs. ((11.5) to (11.7)), it is also implied that the electron density fluctuations along different paths of propagation are not correlated. This is in reasonable agreement with the requirement that the main Fresnel volumes of the neighbour rays do not overlap. The exception is only the case of *o*- and *e*-modes, where cross-correlation is accounted for, because the magneto-ionic split does not result in wide enough displacement between *o*-mode and *e*-mode paths of propagation.

All the three functions from eqs. ((11.5) to (11.7)) can be expressed through the two correlation functions of the complex phase ψ_1. These correlation functions are of the following form:

$$B_{\psi 1}(\omega_1, \omega_2, T_-) = \frac{\pi k_1 k_2}{2} \int_0^{S_0} \frac{ds}{\varepsilon_0(s)} \int d\kappa_n\, d\kappa_\tau\, B_\varepsilon(s; 0, \kappa_n, \kappa_\tau) \exp\left[i\kappa_n(\Delta_n - v_n T_-) + i\kappa_\tau(\Delta_\tau - v_\tau T_-) \right] \cdot$$
$$\cdot \exp\left\{ \frac{i\,(k_1 - k_2)}{2k_1 k_2} \left[\kappa_n^2 D_n(s) + \kappa_\tau^2 D_\tau(s) + 2\kappa_n \kappa_\tau D_{n\tau}(s) \right] \right\} \tag{11.8}$$

$$B_{\psi 2}(\omega_1, \omega_2, T_-) = -\frac{\pi k_1 k_2}{2} \int_0^{S_0} \frac{ds}{\varepsilon_0(s)} \int d\kappa_n\, d\kappa_\tau\, B_\varepsilon(s; 0, \kappa_n, \kappa_\tau) \exp\left[i\kappa_n(\Delta_n - v_n T_-) + i\kappa_\tau(\Delta_\tau - v_\tau T_-) \right]$$
$$\cdot \exp\left\{ -\frac{i\,(k_1 + k_2)}{2k_1 k_2} \left[\kappa_n^2 D_n + \kappa_\tau^2 D_\tau + 2\kappa_n \kappa_\tau D_{n\tau} \right] \right\}. \tag{11.9}$$

Here, $k = \omega/c$, $B_\varepsilon(s;\, 0, \kappa_n, \kappa_\tau)$ is a 3D spatial spectrum of the electron density fluctuations with zero value of the spectral variable, Fourier-conjugated to the variable s along the path. It is also the function of the variable s along the reference ray. Spectral variables κ_n and κ_τ are Fourier-conjugated to the spatial variables q_1 and q_2 lying in the plane perpendicular to the reference ray at each point. Quantities Δ_n and Δ_τ are the components of the vector of the distance between the rays corresponding

to frequencies ω_1 and ω_1, which also depend on s. Additionally, the hypothesis of the «frozen drift» of random inhomogeneities is accepted, so that v_n and v_τ are the components of the frozen drift velocity, also depending on the point along the reference ray, and $T_- = T_1 - T_2$ is the difference slow time. The central slow time T_+ is not involved in eqs. ((11.8) and (11.9)), because of the assumption of the statistical homogeneity of fluctuations. Coefficients D_n, D_τ, and $D_{n\tau}$ are the elements of the matrix $\hat{D} = (\hat{B}^+)^{-1}$, which is the inverse of the matrix $\hat{B}^+$, introduced in Gogin *et al.* (2001). Matrix $\hat{B}^+$ is actually a sum of curvature matrices of the incident field and of the Green function. These are obtained by integrating the corresponding differential equations along the reference ray and also depend on the variable s.

In the numerical calculations, the model of the ionospheric fluctuations is considered as turbulence, having the anisotropic spatial spectrum with the inverse power law of the form as follows:

$$B_\varepsilon(s,\kappa) = C_N^2\left[1 - \varepsilon_0(s)\right]^2 \sigma_N^2(s)\left(1 + \frac{\kappa_{tg}^2}{K_{tg}^2} + \frac{\kappa_{tr}^2}{K_{tr}^2}\right)^{-\frac{p}{2}}. \tag{11.10}$$

Here C_N^2 is a known normalization coefficient. $K_{tg} = 2\pi l_{tg}^{-1}$, where l_{tg} is the outer scale of the turbulence along the geomagnetic field, and $K_{tr} = 2\pi l_{tr}^{-1}$, where l_{tr} is the outer scale of the turbulence across the magnetic field. Function $\varepsilon_0(s)$ is the distribution of the dielectric permittivity of the background ionosphere and $\sigma_N^2(s)$ is that of the variance of the relative fluctuations of the electron density of the ionosphere, both along the reference ray in the 3D inhomogeneous ionosphere. As a result, functions ((11.8) and (11.9)) are of a very high degree of the generality, valid for arbitrary three dimensional models of the background ionosphere and fluctuations of the ionospheric electron density.

All the above-mentioned results permit us to uniquely produce random time series of functions χ_m and S_m in the domain (ω, T), if additionally the cross-correlation (11.7) is also properly accounted for when generating the series. In turn, this permits us to generate random values of phasor $R_m(\boldsymbol{r}, \omega, T)$ in the same domain, and finally to generate random series of a signal propagated through the fluctuating ionosphere employing the appropriate methods of numerical calculation of the integrals in eq. (11.1).

Below we shall present some results of simulation obtained according to the technique developed. All the results have been calculated for a single-hop path 1000 km long oriented to the south from St. Petersburg. The IRI model for July at 14:00 LT was chosen for the transmitter site at St. Petersburg and for the receiver site 1000 km to the south of St. Petersburg. For this path, horizontal gradients of the electron density resulted in a difference of 0.5 MHz in *foF*2 between the transmitter and receiver.

The fluctuations of the ionospheric electron density were characterized by the inverse power law anisotropic spatial spectrum with the spectral index of 3.7, the scale of random inhomogeneities across the geomagnetic field of 3 km and the aspect ratio of 5. The variance of relative fluctuations of the electron density was assumed to be uniform along the path of propagation and equal to 10^{-6}. The hypothesis of frozen drift of random inhomogeneities was utilized with the same horizontal longitude and latitude velocity of 0.5 km/s. The bandwidth of the non-monochromatic transmitted signal was 20 kHz.

For the first step, the oblique sounding ionogram was constructed for the model of the background ionosphere chosen, which indicated possible high angle and low angle *F*- and *E*-mode paths of propagation. In fig. 11.1, the random walk is shown for the phasor corresponding to the *E*-mode propagation, whereas fig. 11.2 demonstrates the same for the phasor of the high angle *F*-mode. Clearly, the spread of possible random values of the phasor on the plot of fig. 11.2 is significantly wider due to the higher density of the background ionosphere at the altitude of the *F*-layer, leading to the higher value of the absolute fluctuations of electron density. As an example, in figs. 11.1 and 11.2 the random walk is calculated with no geomagnetic field, However, similar plots can be produced for the case when the geomagnetic field is present.

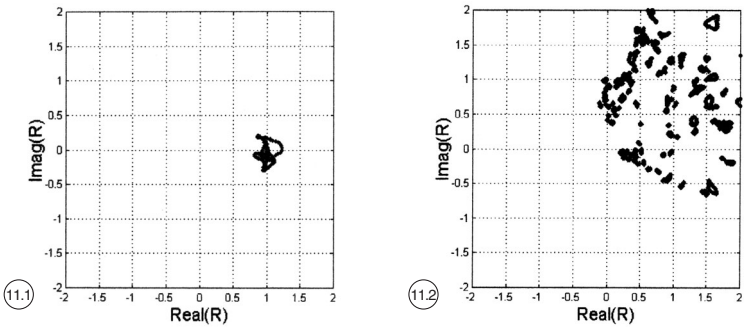

Fig. 11.1. Random walk of phasor for the *E*-mode.

Fig. 11.2. Random walk of phasor for the high angle *F*-mode. The case of stronger fluctuations.

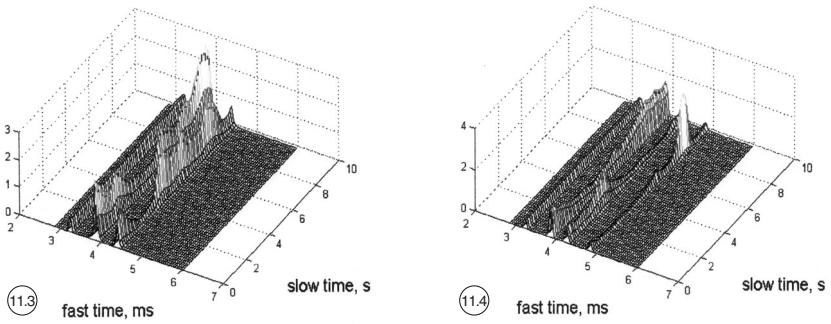

Fig. 11.3. Realization of the received signal plotted in slow time and fast time variables.

Fig. 11.4. Realization of the received signal plotted in slow time and fast time variables calculated for the case of inclusion of the geomagnetic field.

In the following two plots (figs. 11.3 and 11.4) random series of a signal at the location of the receiver are demonstrated. To obtain them, random integrals (11.1) were calculated, having the appropriate distributions of the phasors available, as the function of the fast time (time of flight) for different moments of the slow time.

The plot in fig. 11.3 shows the case without the geomagnetic field, where the contributions of three paths of propagation (high and low *F* and *E*) are well resolved. By contrast with the geomagnetic field present, as in fig. 11.4, contributions due to four paths of propagation are clearly seen. For this case, the high angle *F* ray is split into both *e*- and *o*-mode, whereas this splitting cannot be seen for the other modes.

11.4. Multi-moded wideband scattering functions

The scattering function of a pulsed signal is introduced (Proakis, 1983; Vogler and Hoffmeyer, 1993; Mastrangelo *et al.*, 1997; Gherm *et al.*, 2001a,b) as the appropriate Fourier transform of the

auto-correlation function of the random channel impulse response on the difference slow time variable. Utilising (11.1) the auto-correlation function of a pulsed signal on slow time T can be written as follows:

$$\Psi_U(t, T_1, T_2) = \int P(\omega_1) P^*(\omega_2) \sum_m f_m(\omega_1) f_m^*(\omega_2) \Psi_{Rm}(\omega_1, \omega_2; T_1, T_2) \cdot \\ \cdot \exp\left[ik_1 \varphi_m(\omega_1) - ik_2 \varphi_m(\omega_2) - i(\omega_1 - \omega_2) t\right] d\omega_1 d\omega_2. \tag{11.11}$$

Here the spatial variable $\boldsymbol{r}$ was suppressed and the following relationships have been introduced

$$E_{0m}^{\mathrm{GO}}(\omega) = f_m(\omega) \exp\left[ik\varphi_m(\omega)\right] \tag{11.12}$$

$$\Psi_{Rm}(\omega_1, \omega_2; T_1, T_2) = \left\langle R_m(\omega_1, T_1) R_m^*(\omega_2, T_2) \right\rangle \tag{11.13}$$

Equation (11.12) shows explicitly the amplitude and phase of the field E_{0m}^{GO}, which are calculated for each possible mode of propagation, defined by the model of the background medium. Equation (11.13) is the definition of the two-frequency two-time correlation function of the random phasor $R_m(\omega, T)$.

It is convenient to work with the central and difference variables in the frequency and slow time domains

$$\omega_+ = \frac{1}{2}(\omega_1 + \omega_2), \qquad \omega_- = \omega_1 - \omega_2, \tag{11.14}$$

$$T_+ = \frac{1}{2}(T_1 + T_2), \qquad T_- = T_1 - T_2. \tag{11.15}$$

Utilising new variables in eq. (11.11) and performing Fourier transformation on difference slow time T_-, the following equation for the scattering function (which is sometimes termed as the wideband scattering function) is obtained

$$S(t, T_+, \omega_d) = \frac{1}{2\pi} \int P\left(\omega_+ + \frac{\omega_-}{2}\right) P^*\left(\omega_+ - \frac{\omega_-}{2}\right) \sum_m f_m\left(\omega_+ + \frac{\omega_-}{2}\right) f_m^*\left(\omega_+ - \frac{\omega_-}{2}\right) \cdot \\ \cdot \Psi_{Rm}(\omega_+, \omega_-; T_+, T_-) \exp\left[-i\left(t - t_{gm}(\omega_+)\right)\omega_- + i\omega_d T_-\right] d\omega_+ d\omega_- dT_-. \tag{11.16}$$

Here the summation is performed over all paths of propagation from the source to receiver. The scattering function of the channel $S(t, T_+, \omega_d)$ depends on the Doppler variable ω_d, (Fourier-conjugated to T_-), the group-delay spread t and, generally, on the slow time T_+. The latter dependence vanishes when the random ionospheric fluctuations are assumed to be statistically stationary (the same as in eq. (11.8)). Group delay time $t_{gm}(\omega_+)$ is given by the equation

$$t_{gm}(\omega_+) = \frac{\partial}{\partial \omega}\left[\frac{\omega}{c}\varphi_m(\omega)\right]_{\omega=\omega_+} \tag{11.17}$$

and is calculated for each mode of propagation.

In the framework of the complex phase method, the frequency and time correlation function of the random phasor Ψ_{Rm}, in the integral (11.16), is expressed through the statistical moments of the complex phase (Gherm and Zernov, 1998; Gherm *et al.*, 2001a) as follows:

$$\Psi_{Rm}(\omega_+, \omega_-; T_+, T_-) = V\left(\omega_+ + \frac{\omega_-}{2}\right) V^*\left(\omega_+ - \frac{\omega_-}{2}\right)\left\{\exp\left[\Psi_\psi(\omega_+, \omega_-; T_+, T_-)\right] - 1\right\} \quad (11.18)$$

$$V(\omega) = \exp\left[\left\langle \psi_2(\omega)\right\rangle + \frac{1}{2}\left\langle \psi_1^2(\omega)\right\rangle\right]. \quad (11.19)$$

Function Ψ_ψ is the auto-correlation function of the complex phase with the main term employing the complex phase method by the relationship

$$\Psi_\psi(\omega_+, \omega_-; T_-, T_+) = \left\langle \psi_1\left(\omega_+ + \frac{\omega_-}{2}, T_+ + \frac{T_-}{2}\right)\psi_1^*\left(\omega_+ - \frac{\omega_-}{2}, T_+ - \frac{T_-}{2}\right)\right\rangle. \quad (11.20)$$

Functions ((11.18) to (11.20)) have been studied in detail in Gherm and Zernov (1998) for the case of a horizontally stratified background medium. The scattering function (11.16), also for the stratified background medium, has been studied in Gherm *et al.* (2000, 2001a,b). The extension of the complex phase method, obtained above for the case of a 3D inhomogeneous background medium (Gogin *et al.*, 2001), naturally permits the technique of calculation of the scattering functions to be extended to the general case of a 3D background ionosphere. The statistical moments of the complex phases involved in equations ((11.16), (11.18) to (11.20)) are given through the representations ((11.8) and (11.9)). They are all derived analytically and then calculated numerically for a given model of the background ionosphere.

Figure 11.5 presents the scattering function in the form of a contour plot, calculated according to the outlined technique as the appropriate statistical moment of the signal. The adjacent contours are separated by 5 dB and range from 0 to –30 dB. This calculation was performed for the case of no geomagnetic field.

There is also another possible method of obtaining the scattering function. In this alternative case, it is determined from the random time series, as represented in the plots shown in figs. 11.3 and 11.4. This is a numerical processing of the simulated time series of a signal analogous to what is really done to real experimental data. In figs. 11.6 and 11.7 this form of the scattering function is present-

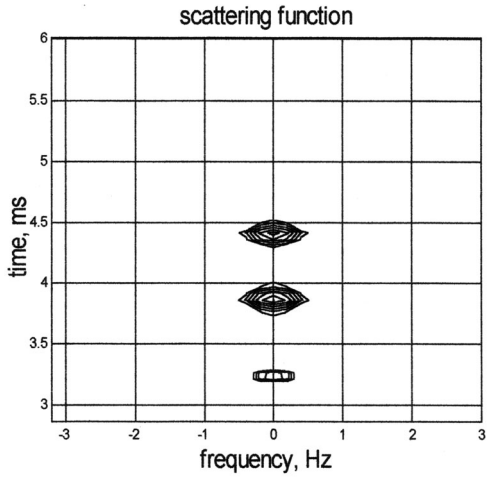

Fig. 11.5. Scattering function calculated theoretically as a statistical moment of the field.

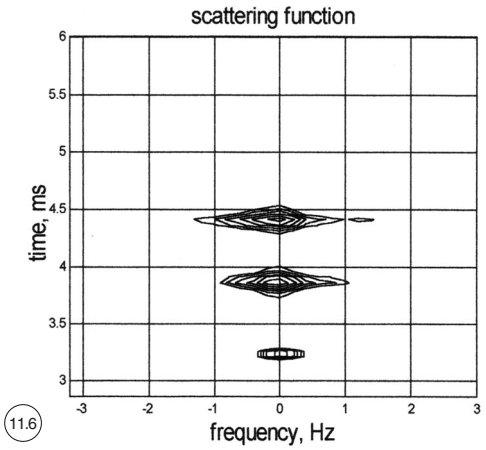

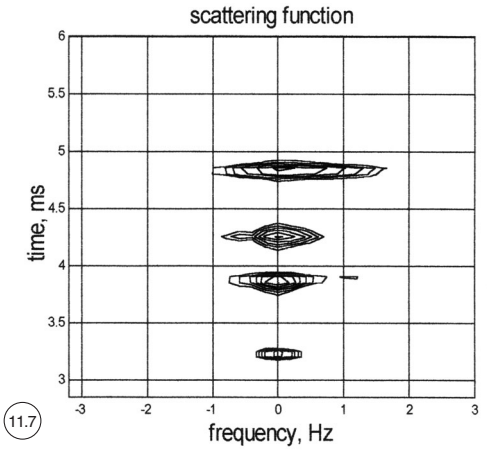

Fig. 11.6. Scattering function determined from the field realizations shown in fig. 11.3.

Fig. 11.7. Scattering function determined from the field realizations for the case when the Earth's magnetic field is taken into account. The uppermost region corresponds to the extraordinary component of the high angle *F*-mode.

ed for the two cases: with and without the effect of the geomagnetic field. The figures are in the form of contour plots where the adjacent contours are separated by 5 dB and range from 0 to –30 dB. Strictly speaking, these plotted values are not statistical moments, but a sort of realization of the scattering function, obtained after the appropriate partial averaging over a finite series of realizations of the signal. In fig. 11.7, where the effect of the geomagnetic field is accounted for, four distinct regions occur, which present four contributions to the full signal which have propagated along the four paths: *E*, low angle *F* and both *o*- and *e*-modes for high angle *F*.

11.5. Conclusions

A wideband HF ionospheric channel simulator has been constructed which is solely based on a physical model of propagation through a time-varying ionosphere. The use of a propagation model including the Earth's field enables the effect of both *o*- and *e*-modes to be included for all layer reflections. Results from this simulation show the very significant effect of irregularities of even modest magnitude and the comparative effects on the variation of received pulse magnitude and pulse width due to background ionosphere dispersion and the fluctuating irregularities. This emphasizes the shortcomings of previous simulation models for which no such stochastic ionosphere model was included. Further, precisely because the simulator is based on a physical model, comparison of experimental results and simulation can also be used to identify the correspondence between physical parameters (*e.g.,* the variance and anisotropy of the electron density fluctuations, orientation of the propagation path to the magnetic meridian, bulk ionosphere motions) with observed channel parameters (*e.g.,* Doppler spread and shift, time delay spread). This in turn will lead to a better characterisation of the propagation channel and thus a more accurate simulator. Such an iteration is not possible for an empirically based simulator. The simulator could also be used to test HF systems and candidate HF modem schemes for various applications, *e.g.,* HF broadcasting (DRM) and spread spectrum systems, both direct sequence and frequency hopping.

REFERENCES

GHERM, V.E. and N.N. ZERNOV (1995): Fresnel filtering in HF ionospheric reflection channel, *Radio Sci.,* **30**, 127-134.

GHERM, V.E. and N.N. ZERNOV (1998): Scattering function of the fluctuating ionosphere in the HF-band, *Radio Sci.*, **33**, 1019-1033.

GHERM, V.E., N.N. ZERNOV, B. LUNDBORG and A. VASTBERG (1997a): The two-frequency coherence function for the fluctuating ionosphere; narrowband pulse propagation, *J. Atmos. Sol.-Terr. Phys.*, **59**, 1831-1841.

GHERM, V.E., N.N. ZERNOV and B. LUNDBORG (1997b): The two-frequency, two-time coherence function for the fluctuating ionosphere; wideband pulse propagation, *J. Atmos. Sol.-Terr. Phys.*, **59**, 1843-1854.

GHERM, V.E., N.N. ZERNOV, H.J. STRANGEWAYS and M. DARNELL (2000): Scattering functions for wideband HF channels, in P*roceedings of the 8th International Conference on «HF Radio Systems and Techniques»*, University of Surrey, U.K., 10-13 July, 2000, *Conference publication No. 474*, 341-345.

GHERM, V.E., N.N. ZERNOV, B. LUNDBORG, M. DARNELL and H.J. STRANGEWAYS (2001a): Wideband scattering functions for HF ionospheric propagation channels, *J. Atmos. Sol.-Terr. Phys.*, **63**, 1489-1497.

GHERM, V.E., N.N. ZERNOV and H.J. STRANGEWAYS (2001b): Scattering functions for multimoded wideband HF channels, in *Proceedings ICAP2001*, April 2001, Exeter, U.K., *IEE Conference Publ. No. 480*, 393-396.

GHERM, V.E., N.N. ZERNOV and H.J. STRANGEWAYS (2002): Multipath effects in wideband fluctuating HF channels, *Acta Geod. Geophys. Hung.*, **37** (2/3), 253-259.

GHERM, V.E., N.N. ZERNOV and H.J. STRANGEWAYS (2003): Wideband HF simulator for multipath ionospsherically reflected propagation channels, in *Proceedings ICAP2003*, April 2003, Exeter, U.K., *IEE Conference Publ. No. 491*, vol. 1, 128-131.

GOGIN, YU.A., V.E. GHERM and N.N. ZERNOV (2001): Diffraction of the wave field on weak inhomogeneities of the dielectric permittivity in a 3D smoothly inhomogeneous medium, *St. Petersburg University Herald, Series 4*, **2** (12), (in Russian).

MASTRANGELO, J.F., J.J. LEMMON, L.E. VOGLER, J.A. HOFFMEYER, L.E. PRATT and C.J. BEHM (1997) A new wideband high frequency channel simulation system, *IEEE Trans. Commun.*, **45**, 26-34.

PROAKIS, J.G. (1983): *Digital Communications* (McGraw-Hill, New York).

STRANGEWAYS, H.J. (2000): Effect of horizontal gradients on ionospherically reflected or transionospheric paths using a precise homing-in method, *J. Atmos. Sol.-Terr. Phys.,* **62**, 1361-1376.

VOGLER, L.E. and J.A. HOFFMEYER (1993): A model for wideband HF propagation channels, *Radio Sci.*, **28**, 1131-1142**.**

ZERNOV, N.N. (1980): Scattering of waves of the SW-range in oblique propagation in the ionosphere, *Radiophys. Quantum Electron.*, **23**, 109-114.

ZERNOV, N.N., V.E. GHERM and H.J. STRANGEWAYS (2002): Modelling of wideband ionospheric HF channels, in *Proceedings 27th General Assembly of URSI*, Maastricht, The Netherlands, *Pap. No. 0785*, pp. 4.